Modeling of the Halloysite Spiral Nanotube

Francesco Ferrante,* Nerina Armata, and Giuseppe Lazzara

Dipartimento di Fisica e Chimica, Università degli Studi di Palermo,

Viale delle Scienze, Parco d'Orleans II, Ed. 17, 90128, Palermo, Italy.

E-mail: francesco.ferrante@unipa.it

Abstract

A computational SCC-DFTB investigation dealing with the structure of hydrated and anhydrous halloysite nanotubes with a spiral geometry is reported. The peculiar characteristics of these systems are described in terms of tetrahedral and octahedral distortions, of hydrogen bonds geometries involving water molecules and the surfaces in the hydrated nanotube, and of the interlayer interactions in the anhydrous one. When the properties of the spiral nanotube are compared with those of the kaolinite sheet, a certain degree of intrinsic disorder in the halloysite systems is revealed, due to the intrinsic nature of the spiral folding. This is particularly evident in the hydrogen bonds network occurring in the hydrated nanotube.

Keywords: hydrated clays, tubular systems, density functional tight binding

Introduction

Halloysite is a clay mineral belonging to the kaolinite group and occurring in nature with platy, spheroidal or hollow tubular shape. The dominant morphology is the multiwalled tubular one

*To whom correspondence should be addressed

which presents sizes between 500-1000 nm in length and 15-100 nm in inner diameter depending on the deposit. The reason of the curving and the rolling up of the flat kaolinite to form multi-layer tubes is still unclear.[1] A spiral-like structure could be clearly imaged by electron microscopy experiments.[2,3] Laboratory scale experiments showed that hydrothermal conditions lead to an increased tendency of $Al_2Si_2O_5(OH)_4$ to crystallize as halloysite than planar kaolinite but to this aim the partial substitution of SiO_2 with GeO_2 is necessary. Despite the success in obtaining the halloysite nanotube, the specific effect that Ge(IV) has on the curvature of the nanosheets to promote nanotubular morphology is still a matter of debate.[4]

Thanks to its peculiar shape, halloysite is considered a promising entrapment system for the loading, the storage and the controlled release of variuos species.[5,6] Moreover, these clay materials are economically viable and enviromentally friendly and, for this reason, competitive with other tubular systems as carbon, polymeric, metal or metal oxide nanotube.[7]

Halloysite is a 1:1 aluminosilicate and its crystal structure can be described as a layer composed by two building blocks: SiO_4 tetrahedra and AlO_6 octahedra with an ideal unit formula $Al_2Si_2O_5(OH)_4 \cdot nH_2O$. Since its discovery, several classification schemes of halloysite have been proposed and for the purposes of this work we chose the one based on the hydration and the interlayer spacing of the system. Namely, halloysite-7Å is the dehydrated form (n=0) characterized by a spacing between two layers of 7.5 Å and halloysite 10Å is the hydrated form (n=2) with an interlayer spacing of 10 Å. The interlayer distance of halloysite 7Å is the same of that observed in flat kaolinite, while the increase of the thickness of the halloysite-10Å is caused to the presence of water molecules.

Several investigations, based on the temperature of water volatilization determined by thermogravimetric analysis, addressed to the characterization of the interlayer water, led to the identification of two types of water molecules: *hole water* molecules, which form hydrogen bonds with basal oxygens of the surface of the SiO_4 sheet and have a molecular HH vector parallel to the surface, and *associated water* molecules, which interacts with both the hole water and hydroxyls of the octahedral sheet and have a molecular HH vector almost perpendicular to the surface nor-

mal.[8,9] The high volatilization temperature for the associated water clearly indicates the presence of strong interactions which are confirmed by hydrogen-isotope exchange experiments in halloysite nanotubes indicating that only one-third of the total hydrogen content can be exchanged at ambient temperature with water vapors.[10] Besides these empirical observation, a detailed picture of the water organization within the HNT structure is not yet depicted.

The investigation of organic and inorganic nanotubes is very attractive also from a theoretical point of view and many efforts have been addressed to the computational study of the structural and electronic properties of these systems. A first attempt to model halloysite nanotubes have made by Guimarães *et al.* who investigated by means of density functional based tight binding method the stability, the electronic and the mechanical properties of single-walled halloysite nanotubes,[11] where of course interlayer water molecules were not considered. Also the theoretical study about the interaction between water molecules and clay materials has been object of a number of studies but, so far, the interest have been addressed towards flat systems as kaolinite or dickite.[12–15]

In this work we report for the first time the modelization of a spiral halloysite nanotube, both in the hydrated and in the anhydrous form. The aim of this investigation is to characterize i) the local structural distortions which must occur to a kaolinite sheet in order to originate a spiral arrangement, ii) the structure of stoichiometric water trapped between the arms of the spiral nanotube, iii) the role of this water molecules as regard the linkage of overlapping arms and iv) the different hydrogen bond networks which water molecules give rise to in the regions between the arms and in the outer silicic surface of the halloysite nanotube.

Models and computational details

The spiral halloysite supercells were fully optimized by using the Self Consistent Charge variant[16] of the Density Functional Tight Binding method as implemented in the DFTB+ code.[17] Slater-Koster parameters which are specific to all the atom pairs occurring in the investigated systems are contained in the so-called MATSCI-0-3 set.[18,19] The approach used in this work has been already

employed for the modelistic characterization of other kinds of non-carbonaceous nanotubes, such as aluminium oxide,[20] imogolite[21] and non-spiral non-hydrated halloysite nanotubes.[11]

The initial geometry of the spiral supercell was built by using a home made program[22] which, exploiting the geometrical and analytical properties of Archimedean spiral, generates a regular spiral lattice by starting from the cell coordinates of kaolinite.

According to Singh and Mackinnon,[23] two limiting directions, depicted in Figure 1, have been chosen for the winding of the hypothetical kaolinite layer from which the spiral nanotube originates. In the first one the winding axis is parallel to the **a** vector, while in the second it is parallel to the **b** vector; these winding directions will be indicated as A- and B-type winding, respectively.

[Figure 1 about here.]

In order to simulate an indefinitely long nanotube, the supercell was replicated along the winding axis by using a cell vector length obtained from the structure of bulk kaolinite. This cell vector length is 5.2 Å for the A-type winding and 9.0 Å for the B-type one. Since this cell vector should not be subjected to sensible strain in the rolling process, it has not been relaxed during geometry optimization. The other two lengths for the simulation box has been chosen equal to 300 Å, thus providing enough empty space to avoid spurious interactions of the spiral nanotube with its periodic replicas.

A total of four models has been considered (Figures 2 and 3), with the following characteristics: the first two models are kaolinite-like (halloysite-7Å; dehydrated halloysite) spiral nanotube with A-type and B-type winding; the third and fourth models are hydrated halloysite (halloysite-10Å) A-type and B-type winding, respectively. For halloysite-7Å a repeating unit of 36 atoms (stoichiometry: $H_{12}Al_4Si_4O_{20}$) has been necessary, which increases to 42 atoms ($H_{16}Al_4Si_4O_{22}$) for the halloysite-10Å case. Since we aimed to model spiral nanotubes with a inner cavity diameter of approximately 5 nm and overlapping arms between one half and one third of revolution, 30 and 50 repeating units have been used for the A-type and B-type winding supercells, respectively, with a spiral phase between 5π and 6.5π. In particular, halloysite-7Å and halloysite-10Å supercells

in the A-type winding are composed by ca. 1100 and 1400 atoms, respectively, and the number of atoms increases to ca. 1700 and 2000 in the case of the corresponding B-type winding supercells. Water molecules in the halloysite-10Å have been located on the silicic surface, following the $Al_2Si_2O_5(OH)_4 \cdot 2\,H_2O$ stoichiometry. The starting position of the two water molecules on the unit cell was chosen so that their orientation on the halloysite surface was the one obtained by Smirnov et al.[12] from molecular dynamics simulations of water adsorption on kaolinite. In particular, the first water molecule was oriented in order to have its HH vector parallel to the surface and to form hydrogen bonds with the oxygen atoms of two adjacent SiO_4 tetrahedra. The second molecule formed only one hydrogen bond and was almost perpendicular to the surface.

[Figure 2 about here.]

[Figure 3 about here.]

Results and discussion

Structures of the halloysite nanotubes

In the following sections the peculiar features of the halloysite nanotube structure will be examined in terms of the octahedral and tetrahedral distorsions resulting from the spiralization of a kaolinite monolayer, of the water geometry in the hydrated systems and of the inter-arms interactions in the anhydrous systems.

We assume throughout that the geometry of water in the different portions of the hydrated halloysite nanotube models is determined mainly by the hydrogen bond networks, whose properties will be detailed in terms of hydrogen bond lengths and orientations. It is worth to note here that these geometrical parameters may be pretty different from the corresponding ones in more simple systems. Usually one can say that shorter distances correspond to stronger non-covalent interactions, but in a complex system such as the one investigated here a certain number of secondary interactions contribute to determine the most stable geometry of the whole aggregate. A distance

between two interacting centers of a molecule can be (usually) larger than expected simply because other interactions compensate the weakening of the main ones.

Octahedra and tetrahedra distortions The curvature of the Archimedean spiral decreases proceeding along the arms from the centre. Distortion of the SiO_4 tetrahedra and the AlO_6 octahedra can be calculated, starting from the relaxed geometry of the halloysite nanotube, by means of the two couples of parameters, λ and σ, defined by the equations:

$$\lambda_t = \frac{1}{4}\sum_{i=1}^{4}\left(\frac{l_i}{l_0}\right)^2 \qquad \sigma_t = \sqrt{\frac{1}{6}\sum_{i=1}^{6}(\theta_i-\theta_0)^2} \tag{1}$$

$$\lambda_o = \frac{1}{6}\sum_{i=1}^{6}\left(\frac{l_i}{l_0}\right)^2 \qquad \sigma_o = \sqrt{\frac{1}{12}\sum_{i=1}^{12}(\theta_i-\theta_0)^2} \tag{2}$$

Here l_0 and θ_0 are the reference bond length and angle for the given polyhedron, respectively, while l_i and θ_i are the actual values in the investigated system. Another geometrical parameter that can be useful to characterize the distortion following the formation of the spiral structure is the angle φ that connects each other the SiO_4 tetrahedra and the AlO_6 octahedra, i.e. the Si-O-Si and Al-O-Al angles. The corresponding distortions, τ, are quantified by

$$\tau_t = \sqrt{\frac{1}{3}\sum_{i=1}^{3}(\varphi_i-\varphi_0)^2} \qquad \tau_o = \sqrt{\frac{1}{6}\sum_{i=1}^{6}(\varphi_i-\varphi_0)^2} \tag{3}$$

where φ_0 is the reference angle taken on the kaolinite ideal crystal.

It turned out that, in all the investigated cases, the analysis of the λ_t and λ_o values is not descriptive, indicating that bond lengths are negligibly affected by the spiralization of the kaolinite sheet. In view of this only the σ parameters will be discussed, by analyzing the difference between their values obtained when the spiral nanotubes are compared with the unfolded kaolinite sheet, investigated at the same level of calculation. As can be noticed by the inspection of the diagrams reported in Figure 4, the unfolded spiral nanotubes, representing an ideal mono-layer slab of kaoli-

nite or hydrated kaolinite, show sensible octahedral σ_o distortions of ca. 8°. These distortions are simply due to the fact that in the kaolinite structure there are no perfect octahedra around the aluminium center; two types of octahedral angles can be identified indeed, with values of ca. 77° and 94° in the 1:3 ratio. The τ_o distortions are negligible, while the tetrahedral σ_t, as well as the inter-tetrahedra τ_t, parameters are small and comprised between 2° and 4°. These values will be taken as reference to analyze the corresponding distortions in the nanotubes.[24]

The diagrams in Figure 4 show the distortions as a function of the polyhedron identifying number, going through the spiral arm from the center outward. The curves here reported for the spiral nanotubes show that aluminium octahedra suffer only small geometrical distortions if the values of σ_o and τ_0 are compared with the corresponding ones in the unfolded nanotube. Both in the A- and B-type winding and regardless of the presence of water in the nanotube, the σ_o parameter has not a regular trend but its variations as a function of the octahedron identifying number are all contained within $\pm 0.5°$ of deviation with respect to the line of the unfolded system. The same trend is observed for the τ_o parameter, whose larger deviation, within 1° from the unfolded nanotube, occur in the halloysite-10Å system. This would mean that the process of spiralization causes only negligible distortions of essentially randomly chosen octahedra, i.e. a sheet formed by aluminium octahedra is already suitable to be folded in a spiral nanotube, even if with a relatively small cavity size as the one investigated here, with a small deformation energetic cost.

A relevant feature is on the other hand revealed for the tetrahedral and inter-tetrahedral distortions σ_t and τ_t. The geometrical deformations of the silicon tetrahedra following the spiralization process have relatively large magnitude, which can reach 8° (σ_t) or 12° (τ_t) of deviation with respect to the corresponding parameters in the unfolded spiral. Further, it seems that, at least in a spiral nanotube with only one third of overlapping arms, the σ_t and τ_t parameters have a variation of the trend every thirty (A-type winding) or fifty (B-type winding) tetrahedral units. In particular, the τ_t distortions roughly repeat their trend periodically, with the largest amplitude at the beginning and an almost monotonic decreasing within the period, irrespective of the type of winding or of the presence of water. The same trend is somehow showed by σ_t for the B-type halloysite-7Å

nanotube, while the same parameter has a more irregular trend for the B-type halloysite-10Å nanotube; finally, when the A-type systems are considered, it turns out that σ_t has values essentially identical to those of the unfolded nanotube for the first half of the spiral arm and shows conversely a repeating trend of distortions for the second half.

This confusing behaviour can be justified by thinking that the nanotubular structures obtained are one of a number of minima existing in the potential energy hypersurface of the investigated systems, but the main information we achieved is that in the process of spiralization of a sheet of interconnected SiO_4 tetrahedra relatively large distortions are localized, with an almost regular fashion, in some regions, hence are not distributed between all tetrahedra.

[Figure 4 about here.]

The structure of water in the hydrated halloysite surface Three kinds of water molecules can be defined in the models of hydrated halloysite nanotubes here investigated (see Figure 3): those between the overlapping spiral arms (*b*-type), those adsorbed on the outer surface of regions where the spiral arms do not overlap (*n*-type) and those adsorbed in the surface of regions where the arms do overlap (*o*-type). Hydrogen bond networks, playing a fundamental role in the determination of the structure of the water component of halloysite-10Å, have been determined as a function of the investigated region of the nanotube. The following geometrical parameters have been considered in order to characterize a hydrogen bond: donor-H distance (d) comprised between 1.5 and 3.15 Å; donor-H-O angle (a) comprised between 145° and 215°. The chosen values defining these ranges permit to identify also hydrogen bond interactions having not optimal orientations.

The *n*-type water molecules are only of modelistic concerns, since they would appear only in a single walled spiral nanotube with a not complete arm overlapping. As a matter of fact, we found only small differences between the *n*-type and *o*-type water molecules, likely attributable to mere polarization effects of the underlying arm in the structure of *o*-type water.

The surface geometries are schematized in Figure 5 and the average geometrical parameters of the interactions, d and a, are collected in Table 1. We report average values because in a spiral

nanotube a strict periodicity exists only in the direction parallel to the nanotube axis; along the arms of the spiral structure, instead, every repeating cell has a geometry slightly different from all the others. Neither a monotonic trend of the geometrical parameters has been observed since, as was detailed in the previous section, tetrahedra and octahedra distortions do not follow a rule and are sometimes disordered, sometimes roughly periodic. Also in the unfolded spiral structure (only *n*-type water molecules are present in this system) there is not a perfect periodicity. It was therefore decided to consider physically affected by the spiralization process only those geometrical parameters whose standard deviation from the mean is sensibly larger than the one of the corresponding parameter in the unfolded structure.

[Figure 5 about here.]

[Table 1 about here.]

In the halloysite-10Å system with A-type winding, the surface water structure can be considered as a grouping of water molecules in pairs. In particular, a water molecule interacts with the halloysite surface and a second molecule forms hydrogen bond with it and with its periodic image. It can be noticed that the interaction between the two water molecules of the pairs is essentially unchanged after the spiralization, and there are only small differences in the hydrogen bond length if *n*-type or *o*-type water molecules are considered. If the differences with the unrolled nanotube are considered, it can be noticed that the spiralization of the kaolinite sheet, inducing a curvature of the surface, favours the approaching of water to the surface (see Table 1). This comes with the generation of a certain degree of disorder, attributable to the not regularly periodic geometry of the spiral. As a consequence, considering the adsorbed water geometry along the nanotube axis direction, there is a sensible elongation of the hydrogen bonds between the water pairs, quantified by the d(5,3*) parameter, where 3* is the periodic replica of the atom labeled 3. In the *o*-type case, the elongation of d(5,3*) is smaller but the interactions between water pairs along the nanotube axis show a larger disorder. The same disorder is mirrored in the OH···O(Si) bond angles, slightly smaller with respect to the unfolded structure, which have standard deviation of 2° and ca. 4°

for the *n*-type and *o*-type water, respectively. It is to remember that the main characteristics of the water adsorption geometry are necessarily affected also by a large number of weak secondary interactions; these are, for example, hydrogen bonds with distances sensibly greater than 3Å. This kind of interactions will not be discussed in details.

The geometry of the surface water in the halloysite-10Å spiral nanotube with B-type winding shows many different features. As it is shown in Figure 5, the hydrogen bond network in this system has a certain degree of complexity, even if also in this case a pair of interacting water molecules can be isolated. The two water molecules do interact one with the other and both with the halloysite surface; one of them forms a strong and ordered hydrogen bond, while one hydrogen atom of the other forms two slightly weaker hydrogen bonds with oxygen atoms of the surface. These latter have variable length along the arms of the spiral, as suggested by the values of the standard deviations, which would mean that the second water molecule is less firmly anchored than the first on the surface. Indeed, when *o*-type water is taken into account, it can be noticed that the underlaying layer has a sensible effect on its hydrogen bond geometry: the second water molecule approaches more definitely one oxygen atom of the surface (d(6,7) is reduced by 0.12 Å while d(6,8) increases by 0.07 Å) and the hydrogen bond between the two water molecules is stretched by ca. 0.18 Å. On the other hand, the d(3,4) and a(2,3,4) parameters, and their standard deviations, are only negligibly affected.

A completely different geometry is adopted by water in the surface of the system originating by unfolding the halloysite-10Å B-type nanotube (a smaller unrolled model, formed by 25 unit cells, has been used for this comparison). Here one can notice that a water molecule enters the center of the surface O-Si-O hexagonal arrangement and forms a weak hydrogen bond with an oxygen atom of the underlying aluminium layer; the average H-bond length, d(6-O′), is ca. 2.62 Å, with a standard deviation of 0.002 Å. The strongest interaction in this case is by far the hydrogen bond between the two water molecules (d(1,2) is 1.89 Å), while the interactions with the upper layer are weakened, being 2.52 Å the average distance between H3 and O4. The degree of disorder of the hydrogen bond network on this surface is essentially zero. It is therefore evident that the process

of spiralization around the B axis has a major effect on the structure of surface water.

The water molecules between the arms of hydrated halloysite The non strictly periodicity of the unit cell along the arms of the halloysite spiral nanotube has sensible effects also on the geometry of the water molecules located between the arms. These water molecules are comprised between an upper layer of aluminium oxide and a lower layer of silicon oxide. In the models here used to investigate the halloysite nanotubes (halloysite-10Å, both A- and B-type) it is possible to recognize twelve pairs of such molecules, if one wants to prevent border effects to enter in the description. In order to temptatively perform a detailed analysis of water arrangement, let use the convention reported in the lower part of Table 2 to describe the way each molecule of the pairs behaves with respect to the halloysite inter-arms surfaces and with respect to the other molecule in the same pair. As already said, secondary interactions, e.g. hydrogen bonds with distances greater than 3 Å or with a orientations outside the considered range, will not be analyzed.

[Table 2 about here.]

Taking a look at Table 2 one can achieve the following information. In the halloysite-10Å system with A-type winding a recurring arrangement of the water molecules is the one where the first molecule of the pair forms a H-bond with the AlO surface and with the second molecule, which in turn forms a hydrogen bond with the lower SiO surface. These water molecules pairs, therefore, establish bridges that connect the two arms of the spiral, by arranging obliquely with respect to the two linked surfaces. Hydrogen bonds are also present between the H_2O molecules in a pair and their images in the adjacent cell originating by the periodic replication along the nanotube axis.

On the other hand, when the spiral nanotube with the B-type winding is considered, it seems that only one water molecule of the pair acts as a link between the arms, by forming hydrogen bond with the upper layer ($H_2O\cdots HO-Al$) and with the lower layer ($HOH\cdots O-Si$). The other water molecule indeed does interact with the first but there are no strong interactions with the surfaces. It is to note here the presence of some too short hydrogen bond (close to 1.6 Å) of the

type $H_2O\cdots HO-Al$, generating a strong loss of symmetry in the inter-arm linkage. Finally, in the halloysite-10Å system with B-type winding there are never interactions between water molecules and their replicated images.

Also in the geometry of water molecules placed between the arms of the spiral nanotube a large degree of disorder exists. This is likely due to the huge number of energetic minima, even relative to local geometries of nanotube portions, which are compatible with the balance between all the leading interactions: hydrogen bonds between water molecules, those between water and the halloysite alumic and silicic surfaces and a large number of secondary interactions.

The anhydrous 7.5Å halloysite When we come to analyze the structure of anhydrous halloysite we must expect major differences with respect to the simpler structure of kaolinite, where the periodicity along the axis perpendicular to the overlapping layers ensures ordered interactions. By going from the last unit cell of the arm toward the first overlapping cell, and neglecting the most external cells in order to minimize border effects, one obtains the trends of Figure 6 corresponding to the inter-arms $AlO-H\cdots O-Si$ hydrogen bonds parameters in the anhydrous 7.5Å halloysite with A- or B-type winding. It can be noticed that the hydrogen bonds in the B-type winding, which are in the 1.88-2.52 Å range (with an average value of 2.085 Å and a standard deviation of 0.184 Å), are sensibly shorter than those occurring in the A-type counterpart, which are comprised in the 2.03-2.76 Å range (with 2.37 Å as average value and 0.23 Å as standard deviation). It is perhaps the case that the loss of stability caused by longer hydrogen bonds in the halloysite A-type nanotube is compensated by the occurring of a large number of interactions of the type $AlO-H\cdots(O-Si)_2$, that is interactions where the same hydrogen atom is shared between two oxygen atoms, forming a stronger and a weaker hydrogen bond (in Figure 6 the H-bond parameters are reported only for the stronger one). Such kind of hydrogen bonds have a large variety of geometries.

[Figure 6 about here.]

In order to evaluate the effect of the spiralization a direct comparison with the kaolinite inter-layer hydrogen bond network structure can be tempted. Kaolinite has been extensively investigated

over the years; to our purpose we will refer to the computational DFT investigation performed by Tosoni *et al.*[25], which report also the experimental results obtained through X-ray diffraction by Neder *et al.*[26] Since the X-ray diffraction techniques leave the hydrogen positions largely undetermined, the hydrogen bonds will be compared in terms of the O···O distances corresponding to the AlO−H···O−Si distances reported in Figure 6. Of course, due to periodicity, for Kaolinite only three distinct O···O distances occur, which describe three different types of hydrogen bonds: 3.088 (calculated: 3.031), 2.989 (2.952) and 2.953 (2.904) Å.[25]

In the anhydrous spiral nanotube, essentially all hydrogen bonds are different from each other. The analysis of the hydrogen bond parameters reveals that the anhydrous halloysite with B-winding seems to have a more interacting arms than the A-winding counterpart. In fact, O···O distances in the B-type systems (2.99 Å in the average with 0.13 Å as standard deviation) are more in line with those measured in the kaolinite system. From the data reported by Tosoni *et al.* it seems that the B3LYP exchange-correlation functional used in that work underestimates the O···O distance by ca. 0.05 Å. If the SCC-DFTB approach used in the present work gives more or less the same description, it can be hypotisized that the hydrogen bond between the arms in the B-winded anhydrous halloysite are only slightly longer than those occurring between the sheets of kaolinite. Further, the B mode of folding eventually permits a more regular distribution of hydrogen bonds. Indeed in the graph of Figure 6 it can be noticed the sloppy repetition of a configuration formed by three hydrogen bonds, two of which have essentially the same length (O···H: ca. 1.90 Å, O···O: ca. 2.85 Å) and the other is longer. The corresponding O···H−O angles reflect the same regularity: two of them are almost identical and the third is much smaller; their values, however, show large variations going along the overlapped arms. The A-type anhydrous spiral nanotube, on the other hand, results with longer hydrogen bonds (the mean O···O distance is 3.26 Å with a standard deviation of 0.21 Å), which, if underestimation is assumed, would indicate that a weakening of the interarms interactions occurs on going from kaolinite to spiral anhydrous halloysite with this kind of winding.

Recently, by means of classical molecular dynamics simulations, it was suggested[27] that the spiral form should be the preferred folding for imogolite when the number of unit cells is of the same order of the one used in the present study. In order to estimate the SCC-DFTB energetics for the spiralization process in our investigated systems we compared the absolute energies of the spiral nanotubes with those of the corresponding unfolded sheets. It turned out that, in the particular case here considered, for the halloysite-7Å system the spiral is almost isoenergetic with the kaolinite single sheet (a stabilization of only 5 kJ mol^{-1} has been calculated). The effect of the water molecules present in the halloysite-10Å structure, on the other hand, amounts to a stabilization of 298 kJ mol^{-1} following the spiralization process. This behaviour can be explained by considering that both halloysite-7Å and halloysite-10Å are stabilized by the formation of hydrogen bonds between the overlapping arms, but the water molecules in the latter, in virtue of their mobility, can easily adapt in order to ensure more efficient interactions.

In a recent investigation on imogolite[28] it was suggested that the driving force for the nanotube formation is the Si-O and Al-O bonds relaxation, which would be constrained in the corresponding unrolled sheet. Also, the hydrogen bonds network occurring in the inner surface of that nanotube would contribute to the stabilization. In the halloysite nanotubes here presented, which are pretty different from the imogolite ones, it seems instead that the stabilization of the spiral structure is mainly due to the hydrogen bonds formed in the interarms region. Indeed, no sensible bond length variations have been noticed while, as suggested by the spiralization energetic of halloysite-7Å, the tetrahedral and octahedral distortions, even if of small sizes, should require energy on the whole. Only when water is present in the nanotube, the hydrogen bonds formation causes a significant stabilization of the system.

Conclusions

A model of spiral halloysite nanotube has been used in a computational investigation aimed to obtain information on the distortions of the kaolinite sheet in the process of nanotube formation, on

the nature of the interarms interaction and on the general structural properties of the stoichiometric water molecules in this spiral aluminosilicate. It turned out that the spiralization of a kaolinite sheet, both in the anhydrous and in the hydrated form, does not seem to cause major distortions of the aluminium and silicon polyhedra, even in a small nanotube as the one investigated here. These distortions are generally uneven, depending on the position of the polyhedron on the spiral arm, but in some cases a sort of periodic regularity can be revealed, as if the spiralization process tended to distribute small distortions in the whole structure instead of concentrate large ones in the inner regions of the arms. It may be moreover expected that in a spiral nanotube with a much larger inner cavity diameter those distortions will be even less evident. In view of this, spiralization of kaolinite should not be an energetically demanding task. On the ground of the energetics here guessed, the water molecules should have a major effect on stabilizing the spiral structure with respect to the unrolled one.

The reported analysis suggests that the spiral limiting winding around the $\vec{b}$ axis originates more ordered hydrogen bonds networks, so that this direction should be favoured for spiralization. On the other hand, it seems a consolidated feature of the present study that the peculiar nature of a spiral nanotube, which is formed by repeating aluminosilicate units whose geometry slightly changes going along the arms, is reflected in a more or less sensible way in a disorder of the interaction geometries involving, for the hydrated system, the water molecules placed on the outer surface and those between the spiral arms or, in the anhydrous case, the direct hydrogen bonds between the spiral arms. In these disorded arrangements, stoichiometric water molecules of the hydrated halloysite seem to interact always in pairs, some of them acting as linkages between the spiral arms. The disorder above reflects necessarily a large number of possible hydrogen bond geometries, corresponding to just as many minima in the potential energy surface of the nanotube. This would suggest, if the transition from an energy minimum to another is hypotesized effortless, that the water molecules between the spiral arms are quite unsettled, so that the interaction between the arms could be seen as a dynamic linkage instead of a static one.

Last to mention, the spiral nanotube models used and relaxed in this work can be taken as the

starting point for more dedicated investigations involving the adsorption of small molecules on the inner or outer halloysite surfaces, or their modifications. As an a example, a suitable replicated spiral supercell can be used to build up a finite nanotube to be studied by using hybrid QM/MM approaches, where a portion which is considered most responsible of a given properties is treated accurately, while the MM is used in order to maintain the spiral framework, avoiding the need to resort to very small, non representative, models of the halloysite surface, whose curvature should be artificially guaranteed by freezing the position of a large number of atoms.

Acknowledgement

This work was financially supported by the FIRB 2012 project (prot. RBFR12ETL5).

Supporting Information Available

Band gaps in halloysite-7Å and halloysite-10Å (spiral and unrolled forms); optimized cartesian coordinates of the supercell for all the investigated nanotubes and unrolled systems. This information is available free of charge via the Internet at http://pubs.acs.org.

References

(1) Joussein, E.; Petit, S.; Churchman, J.; Theng, B.; Righi, D.; Delvaux, B. Halloysite Clay Minerals - A Review. *Clay Min.* **2005**, *40*, 383–426.

(2) Abdullayev, E.; Joshi, A.; Wei, W.; Zhao, Y.; Lvov, Y. M. Enlargement of Halloysite Clay Nanotube Lumen by Selective Etching of Aluminum Oxide. *ACS Nano* **2012**, *6*, 7216–7226.

(3) Lvov, Y. M.; Abdullayev, E. Functional Polymer-Clay Nanotube Composites with Sustained Release of Chemical Agents. *Progr. Polym. Sci.* **2013**, *38*, 1690–1719.

(4) White, R. D.; Bavykin, D. V.; Walsh, F. C. Spontaneous Scrolling of Kaolinite Nanosheets

into Halloysite Nanotubes in an Aqueous Suspension in the Presence of GeO_2. *J. Phys. Chem. C* **2012**, *116*, 8824–8833.

(5) Cavallaro, G.; Donato, D. I.; Lazzara, G.; Milioto, S. Films of Halloysite Nanotubes Sandwiched between Two Layer of Bipolimer: From the Morphology to the Dielectric, Thermal, Transparency, and Wettability Properties. *J. Phys. Chem. C* **2011**, *115*, 20491–20498.

(6) Cavallaro, G.; Lazzara, G.; Milioto, S. Exploiting the Colloidal Stability and Solubilization Ability of Clay Nanotubes/Ionic Surfactant Hybrid Nanomaterials. *J. Phys. Chem. C* **2012**, *116*, 21932–21938.

(7) Lvov, Y. M.; Shchukin, D. G.; Mohwald, H.; Price, R. R. Halloysite Clay Nanotubes for Controlled Release of Protective Agents. *ACS Nano* **2008**, *5*, 814–820.

(8) Costanzo, P. M.; Giese, R. F. J.; Lipsicas, M. Synthesis of Quasi-Stable Kaolinite and Heat Capacity of Interlayer Water. *Nature* **1982**, *296*, 549–551.

(9) Costanzo, P. M.; Giese, R. F. J.; Lipsicas, M. Static and Dynamic Structure of Water in Hydrated Kaolinites. I. The Static Structure. *Clay Clay Min.* **1984**, *32*, 419–428.

(10) Hsieh, J. C. C.; Yapp, C. J. Hydrogen-Isotope Exchange in Halloysite: Insights from Room-Temperature Experiments. *Clay Clay Min.* **1999**, *47*, 811–816.

(11) Guimaraes, L.; Enyashin, A. N.; Seifert, G.; Duarte, H. A. Structural, Electronic and Mechanical Properties of Single-Walled Halloysite Nanotube Models. *J. Phys. Chem. C* **2010**, *114*, 11358–11363.

(12) Smirnov, K. S.; Bougeard, D. A Molecular Dynamics Study of Structure and Short-Time Dynamics of Water in Kaolinite. *J. Phys. Chem. B* **1999**, *103*, 5266–5273.

(13) Tunega, D.; Haberhauer, G.; Berzabek, M. H.; Lischka, H. Theoretical Study of Adsorption Sites on (001) Surfaces of 1:1 Clay Minerals. *Langmuir* **2002**, *18*, 139–147.

(14) Hu, X. L.; Michaelides, A. Ice Formation on Kaolinite: Lattice Match or Amphoterism? *Surf. Sci.* **2007**, *601*, 5378–5381.

(15) Hu, X. L.; Michaelides, A. Water on the Hydroxylated (001) Surface of Kaolinite: From Monomer Adsorption to a Flat 2D Wetting Layer. *Surf. Sci.* **2008**, *602*, 960–974.

(16) Elstner, M.; Porezag, D.; Jungnickel, G.; Elsner, J.; Haugk, M.; Frauenheim, T.; Suhai, S.; Seifert, G. Self-Consistent-Charge Density-Functional Tight-Binding Method for Simulations of Complex Materials Properties. *Phys. Rev. B* **1998**, *58*, 7260–7268.

(17) Aradi, B.; Hourahine, B.; Frauenheim, T. Self-Interaction and Strong Correlation in DFTB. *J. Phys. Chem. A* **2007**, *111*, 5678–5670.

(18) Frenzel, J.; Oliveira, A. F.; Jardillier, N.; Heine, T.; Seifert, G. Semi-Relativistic, Self-Consistent Charge Slater-Koster Tables for Density-Functional Based Tight-Binding (DFTB) for Materials Science Simulations. TU-Dresden 2004-2009.

(19) Frenzel, J.; Oliveira, A. F.; Duarte, H. A.; Heine, T.; Seifert, G. Structural and Electronic Properties of Bulk Gibbsite and Gibbsite Surfaces. *Z. Anorg. Allg. Chem.* **2005**, *631*, 1267–1271.

(20) Enyashin, A. N.; Ivanovskii, A. L. Theoretical Prediction of $Al(OH)_3$ Nanotubes and Their Properties. *Phys. E* **2008**, *41*, 320–323.

(21) Guimaraes, L.; Enyashin, A. N.; Frenzel, J.; Heine, T.; Duarte, H. A.; Seifert, G. Imogolite Nanotubes: Stability, Electronic, and Mechanical Properties. *ACS Nano* **2007**, *1*, 362–368.

(22) The undocumented source of this program is available for non-commercial use on request to the corresponding author.

(23) Singh, B.; Mackinnon, I. D. R. Experimental Transformation of Kaolinite to Halloysite. *Clay Clay Min.* **1996**, *44*, 825–834.

(24) The spikes (with heights of a small fraction of degree) and irregularities appearing in the curves of the unfolded nanotubes in the diagrams of Figure 4 are only computational artifacts. They are due to the fact that the starting geometries for the kaolinite and hydrated kaolinite mono-layers have been obtained just by unfolding the spyral stuctures of the a-type halloysite-7Å and halloysite-10Å, respectively. These irregularities are therefore due to small residual forces still acting on the nuclei of the corresponding tetrahedra and octahedra, and have essentially no importance.

(25) Tosoni, S.; Doll, K.; Ugliengo, P. Hydrogen Bond in Layered Materials: Structural and Vibrational Properties of Kaolinite by a Periodic B3LYP Approach. *Chem. Mater.* **2006**, *18*, 2135–2143.

(26) Neder, R. B.; Burghammer, M.; Grasl, T.; Schulz, H.; Bram, A.; Fiedler, S. Refinement of the Kaolinite Structure from Single-Crystal Synchrotron Data. *Clay Clay Min.* **1999**, *47*, 487–494.

(27) González, R. I.; Ramírez, R.; Rogan, J.; Valdivia, J. A.; Munoz, F.; Valencia, F.; Ramírez, M.; Kiwi, M. Model for Self-Rolling of an Aluminosilicate Sheet into a Single-Walled Imogolite Nanotube. *J. Phys. Chem. C* **2014**, *118*, 28227–28233.

(28) Lee, S. U.; Choi, Y. C.; Youm, S. G.; Sohn, D. Origin of the Strain Energy Minimum in Imogolite Nanotubes. *J. Phys. Chem. C* **2011**, *115*, 5226–5231.

Table 1: Average geometrical parameters characterizing the hydrogen bonds geometry of the water molecules adsorbed on the outer surface of halloysite-10Å spiral nanotubes. Distances in Å, angles in degree; standard deviations are reported in parentheses. Refer to Figure 5 for atomic labeling.

	***n*-type**	***o*-type**
	A-winding[a]	
d(1,2)	1.854 (4)[b]	1.845 (6)
d(3,4)	2.207 (26)	2.195 (19)
d(5,3*)	2.052 (9)	2.021 (28)
a(2,3,4)	127.3 (21)	128.8 (36)
	B-winding	
d(1,2)	2.005 (20)	2.189 (13)
d(3,4)	1.947 (13)	1.941 (10)
d(6,7)	2.024 (45)	1.904 (33)
d(6,8)	2.130 (32)	2.204 (52)
a(2,3,4)	152.4 (29)	153.8 (9)

[a] The corresponding average values for the unfolded halloysite-10Å A-type nanotube are: d(1,2) = 1.847 (1); d(3,4) = 2.267 (2); d(5,3*) = 1.975; a(2,3,4) = 132.8 (5). Border effects in the unfolded structure have been eliminated by considering in the average process only the water molecules located in the inner region of the surface.

[b] Standard deviations for distances have been multiplied by 10^3, those for angles have been multiplied by 10.

Table 2: The hydrogen bonds characterizing the structure of the water molecules pairs between the overlapping arms in the two models of halloysite-10Å. In the lower part of the table the description of the symbolism used is reported. Symbols can be nested and the corresponding H-bond length, in Å, follow in parentheses.

Pair	**A-winding**	**B-winding**
1	A1(2.670), R(1.791)	A[1(1.995)+3(1.886)], Y(2.026)
2	B[2(2.228)/3(2.055)], Y(1.801), R(1.982)	A[1(1.619)+3(2.751)], Y(1.996)
3	A2(1.758), Y(1.939)	A[2(2.200)+3(1.952)], Y(2.123)
4	B[1(2.483)/2(1.924)], Y(1.839)	A[1(2.076)+3(1.906)], Y(2.089)
5	C, Y(1.912)	B[1(1.628)/3(2.599)]
6	B[1(2.437)/3(1.995)], Y(1.818), R(1.897)	A[1(1.885)+3(1.865)], Y(2.138)
7	B[1(2.551)+3(2.498)/1(1.876)]	A[1(1.632)+3(1.844)], Y(1.987)
8	B[1(2.300)/3(1.975)], Y(1.798)	A[1(1.858)+3(1.841)]
9	A2(1.768), Y(1.899)	A[1(1.911)+3(1.892)], Y(2.167)
10	B[1(2.476)/2(2.087)], Y(1.841)	A[1(1.616)+3(2.075)]
11	C, Y(1.967), R(1.952)	A[1(1.865)+3(1.843)]
12	B[1(2.450)+3(2.516)/3(1.982)], R(1.912)	A[1(1.629)+3(1.763)]

Symbol	**Description**
with the arm surfaces:	
A	one H_2O forms H-bond, the other not
B	both molecule of the pair form H-bond
C	no molecule of the pair form H-bond
between water molecules:	
Y	H-bond between the molecules of the pair
R	H-bond with replicated image water
type of hydrogen bond:	
1	$H_2O\cdots HO-Al$
2	$HOH\cdots O(H)-Al$
3	$HOH\cdots O-Si$

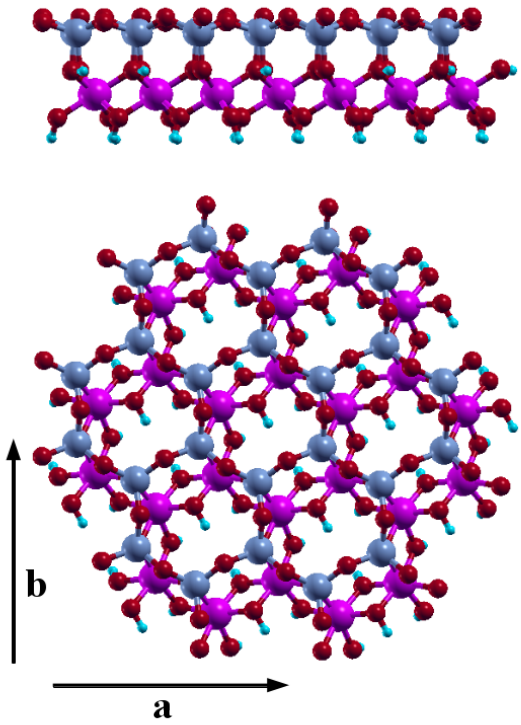

Figure 1: The structure of a kaolinite layer (two views) and the direction of the **a** and **b** cell vectors, parallel to the two limiting winding corresponding to the formation of the A- and B-type spiral nanotubes.

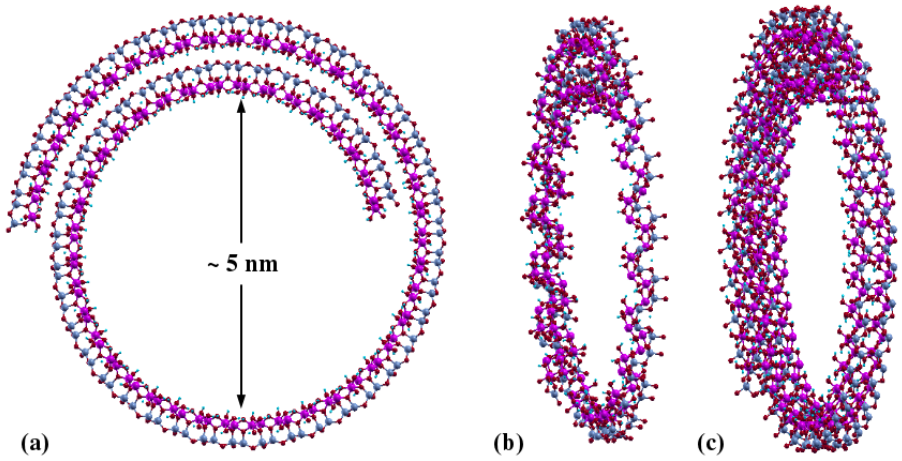

Figure 2: Supercells for the halloysite-7Å nanotube: (a) front view, (b) supercell for the A-type winding, (c) supercell for the B-type winding.

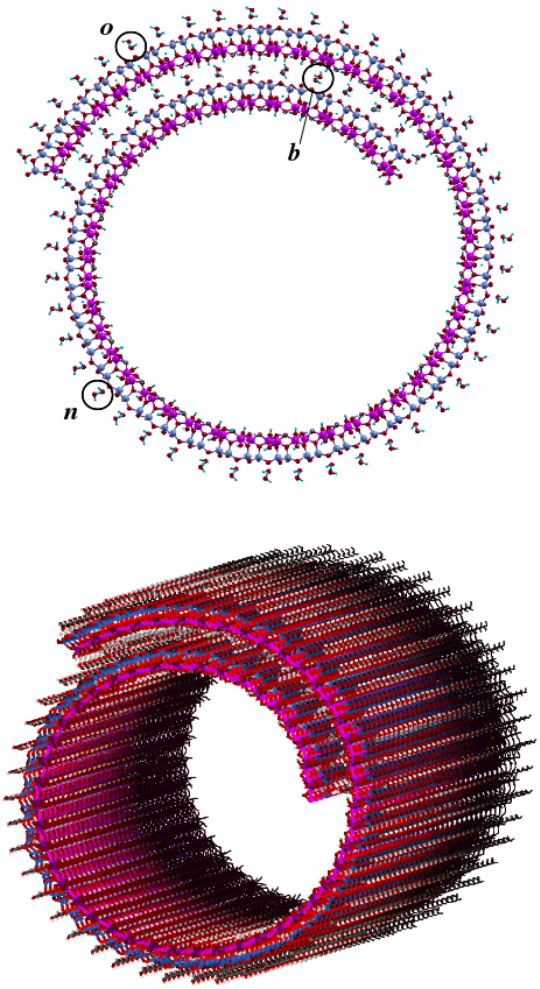

Figure 3: Supercell for the halloysite-10Å nanotube (front view) and schematization of the nanotubular species. Three types of water molecules coexisting in this model are identified by the symbols *b*, *n* and *o*.

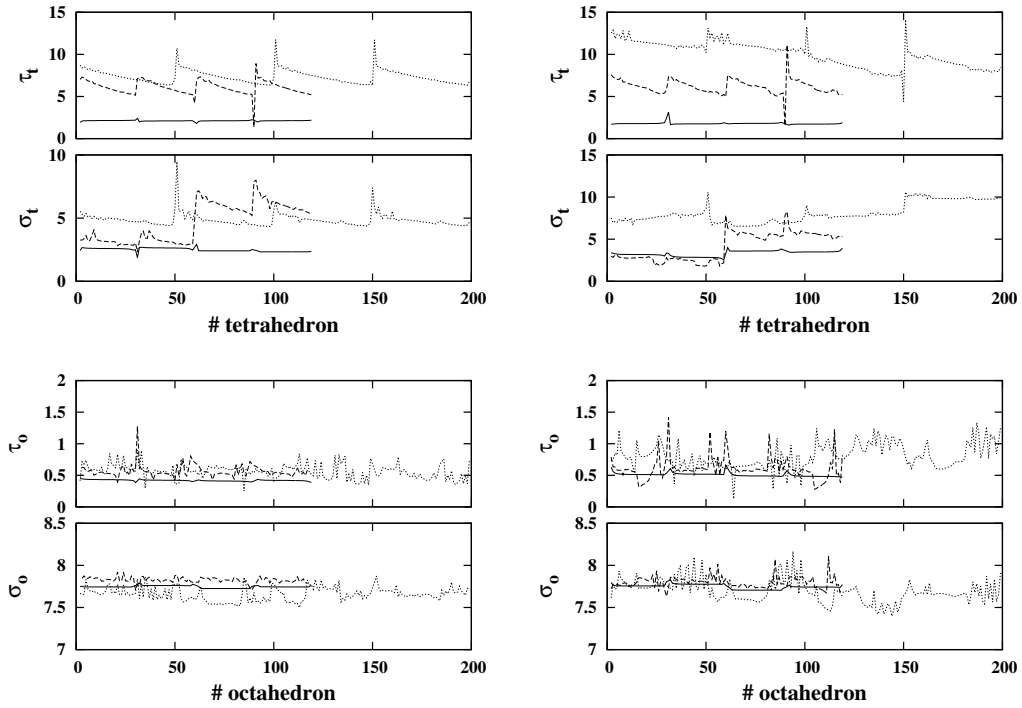

Figure 4: Distortions of the SiO_4 tetrahedra and AlO_6 octahedra as quantified by the parameters defined in equations 1-3. Left panels: halloysite-7Å; right panels: halloysite-10Å. Solid lines: unfolded spiral; dashed lines: spiral nanotube with A-type winding; dotted lines: spiral nanotube with B-type winding.

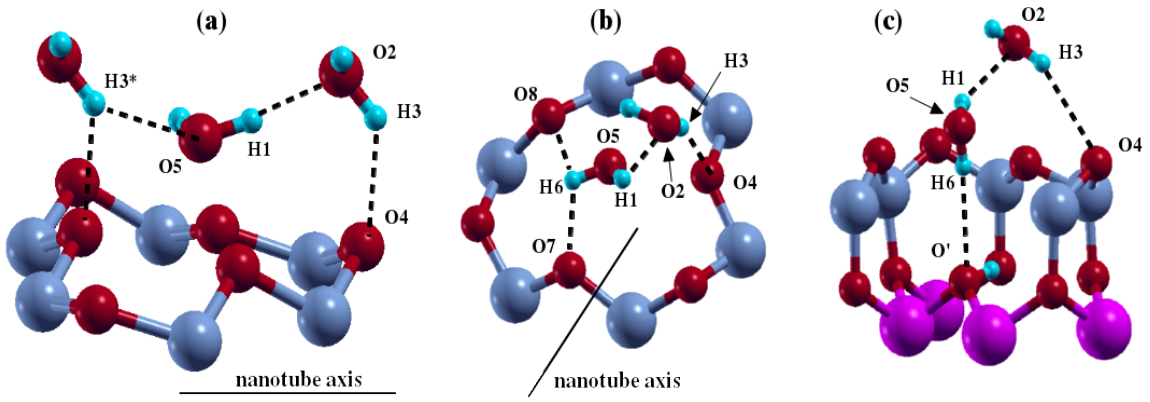

Figure 5: a) The surface water structure in the halloysite-10Å A-type tubular system, which is common to the A-type unfolded spiral; b) Surface water arrangement in the halloysite-10Å B-type spiral nanotube and c) in the unfolded B-type system.

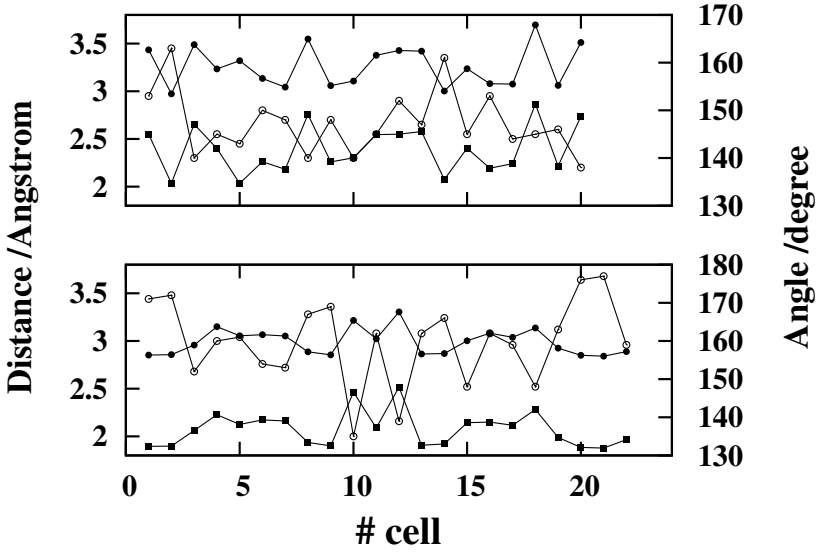

Figure 6: Inter-arms AlO−H···O−Si hydrogen bonds geometrical parameters in the halloysite-7Å spiral nanotubes with A-type (top panel) and B-type (bottom panel) winding. Filled squares: H···O distances, filled circles: O(H)···O distances, empty circles: O−H···O angles.

TOC entry

Modeling of the Halloysite Spiral Nanotube

Francesco Ferrante, Nerina Armata, and Giuseppe Lazzara